Hindawi Publishing Corporation
Journal of Nanomaterials
Volume 2016, Article ID 1537269, 17 pages
http://dx.doi.org/10.1155/2016/1537269

Review Article

Performance Enhancement of Carbon Nanomaterials for Supercapacitors

Amin M. Saleem,[1,2] Vincent Desmaris,[1] and Peter Enoksson[2]

[1]*Smoltek AB, Regnbågsgatan 3, 41755 Gothenburg, Sweden*
[2]*Micro and Nanosystems Group, EMSL, Department of Microtechnology and Nanoscience, Chalmers University of Technology, 41296 Gothenburg, Sweden*

Correspondence should be addressed to Amin M. Saleem; amin@smoltek.com

Received 27 May 2016; Accepted 26 June 2016

Academic Editor: Zeeshan Khatri

Carbon nanomaterials such as carbon nanotubes, carbon nanofibers, and graphene are exploited extensively due to their unique electrical, mechanical, and thermal properties and recently investigated for energy storage application (supercapacitor) due to additional high specific surface area and chemical inertness properties. The supercapacitor is an energy storage device which, in addition to long cycle life (one million), can give energy density higher than parallel plate capacitor and power density higher than battery. In this paper, carbon nanomaterials and their composites are reviewed for prospective use as electrodes for supercapacitor. Moreover, different physical and chemical treatments on these nanomaterials which can potentially enhance the capacitance are also reviewed.

1. Introduction

One- and two-dimensional carbon nanomaterials such as carbon nanotubes, carbon nanofibers, and graphene have been exploited for a long time owing to their extraordinary chemical, mechanical electrical, and thermal properties and are therefore investigated extensively as thermal heat sink, electrical interconnects [1], field emitter, high mechanical strength composites [2], energy storage [3], and high frequency applications [4]. The carbon nanomaterials also have high specific surface area; the theoretical surface area of closed tip CNTs and graphene is 1350 m^2/g and 2630 m^2/g, due to high aspect ratio of CNTs and thin single layer of graphene sheet, and they are therefore recently investigated extensively as electrode materials for supercapacitor (SC) because of proportionality of capacitance versus electrode surface area given as [5, 6]

$$C \propto \frac{A}{d}. \quad (1)$$

SC is a class of energy storage devices, whose technology bridges the gap between conventional energy storage technologies such as parallel plate capacitor and battery by combining parts of their respective working mechanisms. In SC, the electrodes are usually immersed in electrolyte like a battery and charges from electrolyte and electrode accumulate electrostatically at the electrode/electrolyte interface like in parallel plate capacitor. The SC does not have any dielectric; however, the two layers of charges are separated by a monolayer (called Helmholtz layer) of solvent molecules which is considerably thin (0.5–1 nm) resulting in high capacitance [7].

The SC has outstanding features such as quick store/release of energy, about one million charge/discharge life cycles, and ecofriendliness. The power density of supercapacitor (100 kW/kg) is much higher than the conventional battery; however, the energy density (10 Wh/kg) is an order of magnitude less than battery (100 Wh/kg). The power density (specific power) and energy density (specific energy) of different energy storage/conversion technologies are given in the Ragone plot; see Figure 1.

SC is predicted to have application in portable electronic, hybrid vehicles, heavy machinery, airborne places, and even in satellite. Moreover, SC can be helpful in enhancing the life of existing batteries. In fact, the demand of high power pulses from traditional batteries causes deterioration and shortens

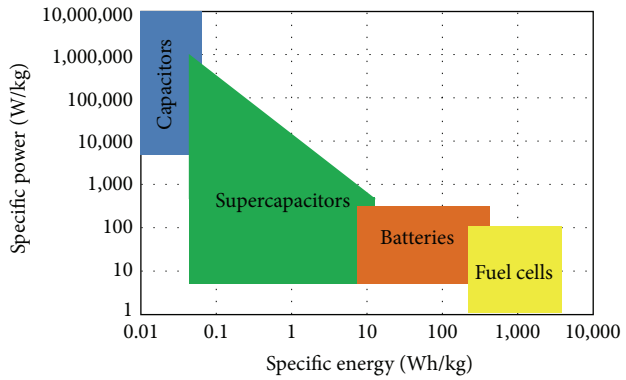

Figure 1: Specific energy and specific power plot of energy storage and conversion devices.

the lifetime. However, on coupling it with SC, the life will be increased by providing pulses from SC and the average power by the battery [8]. Furthermore, existing SC with moderate energy density can be used at place requiring high power for short time such as to close a bus door, initial push to hybrid bus, and quick response of backup energy source such as uninterruptible power supply (UPS); however, the ambition is to use supercapacitor as an independent source of energy to drive buses by enhancing energy density further [9–11].

Supercapacitors are divided into two categories based on their energy storage mechanism such as electric double-layer capacitor (EDLC) and pseudocapacitor. In EDLC, the energy is stored by the electrostatic adsorption of charges on the surface of the electrodes similar to parallel plate capacitor. In contrast, the energy in pseudocapacitor is stored by the reversible Faradaic redox reaction taking place at the surface of the electrodes. The fast charge transference in Faradaic redox reactions than the chemical reaction in the battery results in higher power density than battery and less than EDLC. The electrostatic adsorption/desorption in EDLC is a physical and very fast process resulting in high power density as well as long life cycles unlike batteries which have lower power density and shorter life cycle due to slow chemical reaction and consumption of the electrode by the chemical reactions.

The energy and power of supercapacitor are given in (2); however, specific energy (energy density) and specific power (power density) can be obtained by dividing (2) by mass, footprint area, or volume of electrode materials. The energy depends on the capacitance (C) and operating voltage (V) window or cell voltage whereas the power depends on internal resistance as well which is the sum of equivalent series resistance (ESR) and charge transfer resistance (R_{ct}) where ESR is the sum of electrode materials resistance, bulk electrolyte resistance, and the contact resistance between electrode and current collector [12]:

$$\text{Energy} = \frac{CV^2}{2}, \qquad \text{Power} = \frac{V^2}{4R}. \tag{2}$$

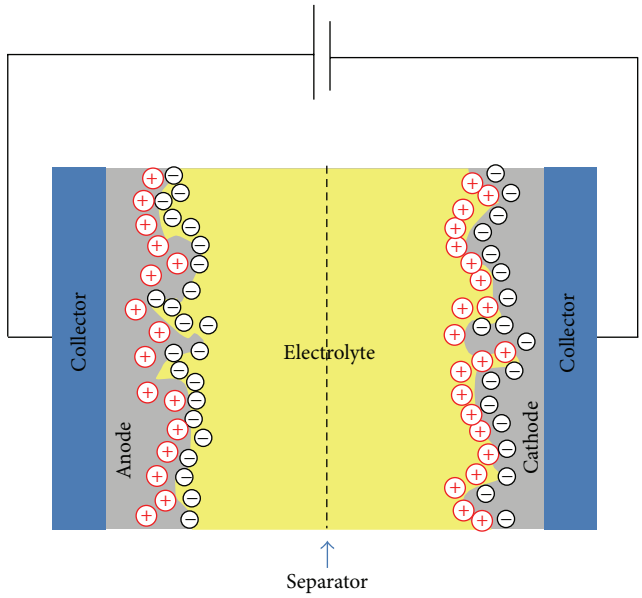

Figure 2: Working principle of supercapacitor.

The energy density is directly related to the surface area of the electrodes materials which advocates carbon nanomaterials as candidate for electrode due to high specific surface area. However, the extraordinary electrical properties of the carbon nanomaterials contribute to reducing overall resistance thus resulting in higher power density of supercapacitor. The power density can be further increased by using electrolyte with high electrical conductivity and larger operating voltage window. The working principle of supercapacitor is shown in Figure 2.

2. Electrolytes

The electrolyte is the main source of ions in the SC and it also defines the cell voltage of SC. In fact, an electrolyte has a particular voltage operating window and it decomposes when operated beyond this window creating gases in the SC. Beside wide operating window, an electrolyte should have high conductivity, low viscosity to access small pores, chemical stability (should not react with the electrode material), easy availability, and cost effectiveness. Different types of electrolytes such as aqueous, organic, and ionic liquid electrolytes are used and properties for typical examples are shown in Table 1. The aqueous electrolytes are highly conductive with smaller ions size which can penetrate inside small pores to access maximum surface area; however, the operating voltage window of these electrolytes is low around 1 V which gives low energy and power density. The low operating voltage of aqueous electrolyte is limited due to the water decomposition voltage of 1.23 V [13]. In fact, the operating voltage window of aqueous electrolyte is defined by the pH value. The commonly used aqueous acidic and basic electrolytes such KOH and H_2SO_4 have high H^+ and OH^- concentration which limits the voltage window [14]. However, the operating voltage can be increased by using neutral electrolytes with low H^+ and

Table 1: Properties of different electrolytes [23].

Electrolyte	Cost	Toxicity	Ion	Ion size (nm)	Pseudocapacitance
Aqueous	Low	Low	K^+	0,26	Yes
			HSO_4^-	0,37	
Organic	Medium/high	Medium/high	Et_4N^+·9ACN (solvated)	1.30	No
			Et_4N^+·9ACN (bare cation)	0,67	
			BF_4·9ACN (solvated)	1.16	
			BF_4·9ACN (bare cation)	0,48	
Ionic liquids	High	Low	EMI^+	0,76 × 0,43	No
			TFSI	0,8 × 0,3	

OH^- concentration and also by appropriate doping of the electrode. In fact, the hydrogen gets stored into the defect domains of electrode materials and results in lower water decomposition voltage [15]. The voltage window of more than 1.6 V from aqueous Na_2SO_4 electrolyte is obtained by doping carbon electrode with oxygen [16, 17]. Even a high operating voltage of 2.4 V is obtained by nitrogen doping of carbon based electrode [14].

The organic electrolytes have higher operating window than the aqueous electrolyte from 2.4–2.8 V. However, they have low conductivity and larger ion size. The larger ions cannot penetrate inside small pores causing a loss in surface areas resulting in low capacitance; however, the low conductivity causes power loss.

Ionic liquids (ILs) electrolytes have high operating voltage window (3.7 V) and ions size smaller than organic electrolyte resulting in even higher energy density. The ILs can function in wide range of temperature because of the absence of the solvent. The eutectic mixture of ILs has been shown to work both at very low temperature (−50°C) and high temperature (80°C) [18]. The ionic liquids electrolytes are expected to fulfill the increasing demands of the supercapacitor industry.

The aqueous electrolytes are a suitable choice for microporous electrodes. However, by optimizing the pores sizes, electrolytes with larger operating voltage can enhance the energy density. The energy density of mesoporous carbon nanofiber is about 16–21 Wh kg^{-1} in aqueous electrolyte and can be increased to 58.75 Wh kg^{-1} in organic electrolyte after optimizing pore size [19].

3. Chemical Vapor Deposition

Chemical vapor deposition (CVD) technique is the most frequently used due to low temperature, controlled location, and also vertically aligned growth of carbon nanotubes/nanofibers. The controlled growth location feature attracted the industry for field emitter display, interconnects, thermal interface materials, and AFM tips applications. The growth of CNTs requires transition metal catalyst to be patterned on the substrate for controlled growth of CNTs.

During the CVD growth, carbon containing gases decomposes into carbon precursors which adsorb on catalyst surface, diffuse into or along the surface of the catalyst, saturate catalyst, and finally precipitate as carbon nanotubes. The schematic diagram of growth of carbon structures is shown in Figure 3. Two types of CVD processes are used depending on the source of energy such as thermal CVD and plasma CVD. The heat is the main source of energy in thermal CVD for growth. The substrate with patterned catalyst is heated to growth temperature to activate catalyst and also to dissociate the carbon containing gases on the catalyst. Thermal CVD is now a primary method for the growth of bundles of vertically aligned CNTs at around 700°C.

In plasma enhanced CVD (PECVD), the additional energy is provided by plasma along with thermal energy which helps to reduce the overall growth temperature. PECVD is subdivided into further types depending on the type of plasma used and named after the type of plasma such as such as microwave (MW-PECVD), radio frequency (rf-PECVD), and direct current (DC-PECVD). PECVD is used to grow both CNFs and CNTs; however, CNFs are frequently grown. Among all PECVD techniques, DC-PECVD is used to grow vertically aligned carbon nanofibers (VACNFs). Single VACNFs or bundle of VACNFs can be grown using this technique where the vertical alignment is provided by the electric field between CNFs and anode. VACNFs can be grown at CMOS (390°C) compatible temperature for on-chip application such as on-chip capacitor and on-chip interconnects [1, 3].

4. Electrospinning

Electrospinning is used to make nonwoven web of polymer carbon fibers using viscoelastic properties of polymers. It has received wide interest from both academia and industry due to versatility, cost effectiveness, and simplicity. For electrospinning, a syringe is filled with polymer which is ejected from the needle of the syringe with certain volume rate. High positive voltage 10–30 kV is applied to polymer with respect to grounded collector and the positive voltage creates ions in the droplet coming from syringe needle. When the electrostatic field overcomes the surface tension of the polymer droplet, the polymer gets elongated having few micron diameter and is deposited on the collector. The field is adjusted to critical field, for certain viscosity of polymer, to keep the certain critical chain entanglement to make fibers, however, higher than critical field causes spitting of polymer and lower field causes beading in the fibers [21]. The flexibility of the method not only makes polymer fibers but

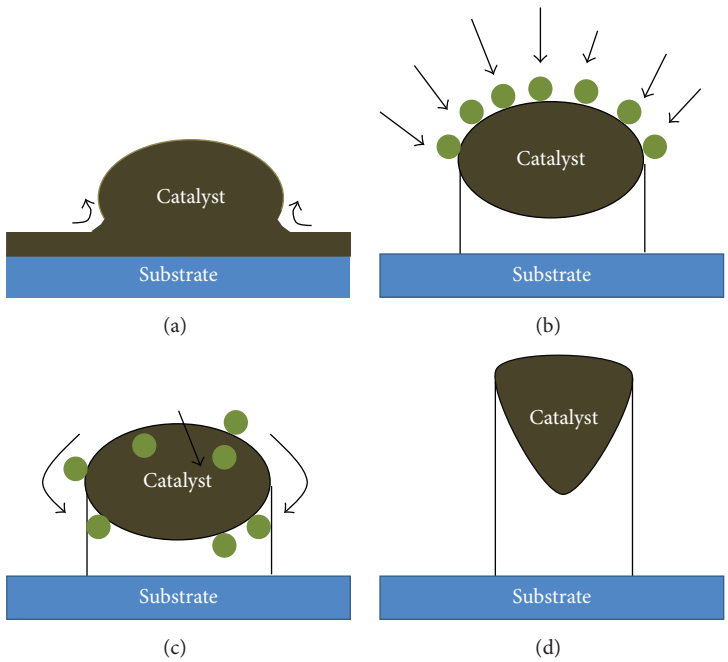

Figure 3: Growth mechanism of carbon nanofiber [20].

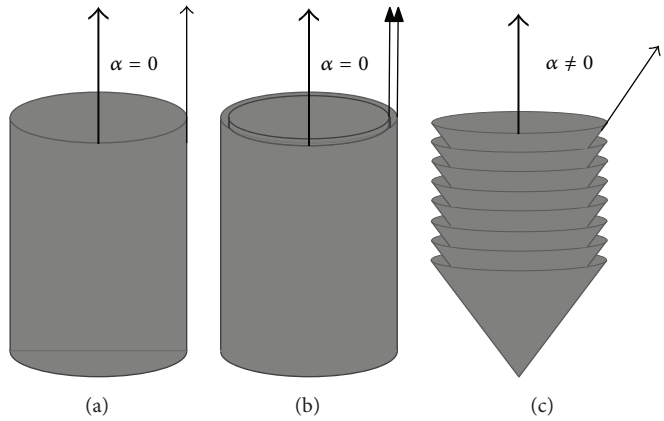

Figure 4: Schematic diagram of (a) single-walled and (b) multiwalled carbon nanotubes and (c) carbon nanofibers.

also can be used to make composite by immersing carbon nanomaterials in polymers [22].

5. Electrode Materials for Supercapacitor

Different types of materials such as activated carbon, templated carbon, carbon nanotubes, carbon nanofiber, graphene, carbon nanomaterials composites, and carbon-metal oxides composites are used as electrode for supercapacitor. However, one- and two-dimensional carbon nanostructures such as carbon nanotubes, carbon nanofibers, graphene, and their composite are focused on here.

5.1. Carbon Nanotubes. Carbon nanotubes are formed by rolling up of one or more than one graphene sheets into concentric cylinder in which the graphene sheet runs through the whole length of carbon nanotube as shown in Figure 4. They are extraordinary materials with excellent thermal, mechanical, and electrical properties. The thermal conductivity of CNTs along the axis (about 3500 W/mK at room temperature) is eight times higher than copper [70] and can carry electric current density three times higher than copper [71]. Mechanically strong CNTs have Young's moduli and tensile strength of 1 TPa and 63 GPa, respectively, many times higher than steel [72]. Because of these properties, carbon nanotubes are studies for many types of applications such as field effect transistors [73–76], interconnects [77, 78], chemical sensors [79], and gas [80] sensors and also as thermal interface materials [81]. In addition, CNTs also have very high aspect ratio with diameter ranging from 1 to 20 nm and length up to few centimeters thus providing high surface area [82]

which makes it an interesting material for hydrogen storage and supercapacitors [83]. Carbon nanotubes are made using arc discharge method, laser ablation, and chemical vapor deposition. Arc discharge and laser ablation produced higher quality CNTs at high temperature (>1000°C) and were therefore the core choices to study the fundamental properties of CNTs. However, they have drawbacks of requiring costly purification methods, lacking the control on growth location, and of course very high growth temperature [84–87].

CVD is the frequently used method nowadays resulting in a variety of CNTs that can be achieved, such as single-walled, double-walled, and multiwalled CNTs, controlled location, and vertically aligned, lying down, short and long, cheap, and quick growth. Recently, bundles of vertically aligned carbon nanotubes are grown at controlled location on silicon substrate using thermal CVD at 700°C in 3 minutes for waveguide application [88]. Catalyst is required to grow CNTs which is either deposited on the substrate or floated in the gases. Floating catalyst CVD method can fulfill the industrial demand because of its ability of economical mass production and controlled structured growth of CNTs [89]. In this process, the catalyst and carbon source such as ferrocene and ethanol are mixed with certain ratio and introduced in the chamber with certain pumping rate. Long ropes of both single-walled and multiwalled carbon nanotubes are obtained. The CNTs ropes of length 5 cm to 6 ft are made by floating catalyst [90, 91].

Long CNTs can also be grown in short time by introducing water in thermal CVD. CNTs of length 2.5 to 7 mm are grown in 10 minutes to 2 hours using WA-TCVD [92–94]. The growth time however is very long but can be shortened by optimizing the parameters further. The thumb rule behind the very long CNTs growth is to keep the catalyst active. The activity of catalyst reduces by the deposition of amorphous carbon. The water vapors hinder the amorphous carbon deposition on the catalyst and keep the catalyst active for longer time. In addition, CNTS grown by WA-TCVD also have high aspect ratio, purity, improved wall structure, alignment, higher growth rate, and longer height [95]. Longer CNTs can be grown by optimizing the growth parameters even without using water. 9 mm long CNTs were also grown by optimizing catalyst reduction time with hydrogen. The mixture of helium and hydrogen and C_2H_4 was used to grow CNTs at 750°C temperature for 10 hours.

The extraordinary properties of CNTs and especially their high surface area make them efficient electrode materials for energy storage purpose. CNTs have narrow distribution of pores due to vertical alignment and most of the surface area is due to the mesopores which help the electrolyte to access all available surface areas. Mesopores also provide the liberty to use electrolytes independent of molecular size.

The carbon nanotubes were used as electrode by using chemically stable binder which does not dissolve in the electrolyte and keep CNTs together but offers less specific surface area because of micropores closing and extra weight of binder. The electrode made from MWCNTs and SWCNTs with PTFE and PVDF binder give surface area of 100 and 130 m^2/g [96, 97]. Similarly, Picó et al. used the arc discharge grown SWCNTs with surface area 236 m^2/g and bound them using PVDF binder and got a specific capacitance of 30 F/g in 6 M KOH electrolyte [29]. The pore size plays an important role in the specific capacitance and the micropores (<2 nm) enhance the surface area and thus capacitance. The aqueous electrolytes can penetrate in the micropores of certain size; however, they cannot penetrate in smaller micropores. In order to utilize the maximum of surface area for capacitance, the ion size of electrolyte should fit in maximum range of pore distribution in electrode thus resulting in limited options of electrolyte; nevertheless, mesopores of vertically aligned carbon nanotubes (VACNTs) provide the solutions of pores related problem. Vertical alignment allows the usage of organic electrolytes having larger ion size but with higher operating voltage window resulting in higher energy and power density. The alignment helps to ease the diffusion of electrolyte to access all the pores of electrode to enhance capacitance and hence power density by reducing resistance (R).

The CNTs can be directly grown or transferred on the current collector which provide good electrical contact between CNTs and current collector. VACNTs were directly grown on silicon chip and a specific capacitance of 47 F/g was obtained in 1 M KOH [98]. Furthermore, VAMWCNTs were grown on silicon substrate and later transferred on double sided tape after gold coating which gave specific capacitance of 440 F/g in ionic liquid electrolyte ([EMIM][Tf_2N]). High energy and power density of 148 Wh/kg and 315 kW/kg were also obtained due to larger voltage window of the electrolyte [40]. Since 2/3 of the produced CNTs are semiconducting when grown as bundle, CNTs have limited electrical conductivity and thus poor energy storage performance. Nevertheless, mesopores help conformal coating of CNTs, which enhance the electrical performance of electrode. The CNTs were coated with titanium nitride and areal specific capacitance of 81 mF/cm^2 was obtained in 0.5 M H_2SO_4 electrolyte which is 5 times the areal specific capacitance of bare carbon nanotubes (14 mF/cm^2) and many folds higher than bare TiN (0.2 mF/cm^2) [99]. Furthermore, supercapacitors are also investigated for ac line filtering which can filter the signals below certain frequency. High conductivity and mesoporosity of electrode can give high areal specific capacitance at high frequency. SWCNTs films were obtained from chlorosulfonic acid dispersion and put on gold coated stainless steel. The areal specific capacitance of 601 $\mu F/cm^2$ is obtained at 120 Hz with phase angle −81° and retained 98% of capacitance after one million cycles [100]. Again, SWCNTs are used with organic electrolyte [1 M $TEABF_4$] with 2.5 V operating window and got the areal specific capacitance of 282 $\mu F/cm^2$ at 120 Hz for 298 nm thick CNTs film. It is shown that the capacitance increases with the increase in film thickness from 53 to 298 nm and decreases with further increase in film thickness due to increase in the pore length [101].

Moreover, solid state capacitors were also fabricated which can be used even at higher frequency. CNTs are conformally coated with Al_2O_3 dielectric and top metal deposition. The volumetric specific capacitance of $C = 23\ mF/cm^3$ at 20 Hz and $C = 6\ mF/cm^3$ at 100–20 kHz is obtained [30]. SCs are made even for higher frequency by

conformal coating of MWCNTs with Al_2O_3 dielectric and TiN using atomic layer deposition technique and achieved the areal specific capacitance of 25 nF mm^{-2} with operating frequency up to 1 MHz [102].

The surface area and conductivity of CNTs can be improved using different treatments such as activation, functionalization, doping, and opening of tips and side walls. The area of as-grown SWCNTs increased from 1300 m^2/g (theoretical surface 1350 m^2/g) to 2240 m^2/g by opening the tips and side walls using heat treatment in dry air at 525°C. The surface area obtained was close to theoretical surface area with inner surface area 1180 m^2/g and outer surface area 1060 m^2/g. The specific capacitance and energy density increased to 114 F/g and 24.7 wh/kg as compared to as-grown CNTs (73 F/g and 16 Wh/kg) [5]. However, to have maximum capacitance, the windows size of side walls should be optimized to size of ion in the electrolyte.

In addition to tip opening, the surface area can be increased by the activation process, which can be done by physical and chemical treatment of CNTs. Frackowiak et al. grew two types of MWCNTS by (a) Co supported on silica and (b) Co solution and then removed the tip by treating with the mixture of hydrochloric acid and nitric acid and activated them with KOH at 800°C temperature under argon flow. The surface area of the MWCNTs on silica substrate increased more than two times (from 430 m^2/g to 1035 m^2/g) whereas the surface area from Co solution increased 4 times (from 220 m^2/g to 885 m^2/g). The specific capacitance increased 5 times after activation (from 10–15 F/g to 90 F/g in KOH electrolyte) [39].

The specific capacitance was also increased by introducing some pseudocapacitance in the CNTs based electrode and this was done by functionalizing the CNTs with an oxygenated group or by nitrogen doping; however, the power density decreased due to a slow redox reaction at the surface. VASWCNTs grown on carbon paper were oxidized by electrochemical method in HNO_3 and the specific capacitance increased from 75 F/g to 158 F/g in an ionic liquid electrolyte; however, power density decreased from 987 kW/kg to 563 W/kg [36].

Moreover, the specific capacitance of 440 F/g with a high energy density of 148 Wh/kg is obtained by opening tips and oxidizing VAMWCNTs using oxygen plasma [40]. The plasma treatments have many positive impacts on CNTs for energy storage such as opening the walls, functionalization, and of course making these structures more hydrophilic because of functionalization. Recently, MWCNTs were functionalized with two types of plasma: (a) microwave plasma, in addition to heat treatment at 500°C in air, and (b) RF oxygen plasma treatment. The contact angle of droplet of 1 M Na_2SO_4 aqueous solution decreased from 113.84° to 36.48° and 19.87° for microwave and RF plasma treated MWCNTs illustrating the hydrophilic properties after plasma treatment. The increase in value of I_D/I_G and AFM proved the existence of window in the walls as well where I_D and I_G are the Raman peaks intensities of defects and graphitization in graphitic materials and their ratio describes the roughness in the graphitic materials. Substantial increase specific capacitances from 61.5 F/g to 214 F/g and 238 F/g were obtained [38]. Nevertheless, the specific capacitances of CNTs based supercapacitors are summarised in Table 2.

5.2. Carbon Nanofibers. Carbon nanofibers (CNF) are fabricated in many ways; however, here CNFs made from chemical vapor deposition (CVD) and electrospinning are discussed. CVD grown CNFs are made by curved graphite layers stacked on top of each other forming cup or cone shaped layers. The stacked cone and cup structures are named as herringbone and bamboo type CNFs having an angle between the CNF axis and graphite walls as shown in Figure 4(c). A weak interplane van der Waals binding between cones makes CNFs weaker than CNTs. Depending on CVD growth technique and measurement method, the CNFs have different properties which are given in Table 3.

CNFs fabricated by electrospinning method are core-shell structures and are in the form of nonwoven mats. These are extensively investigated as electrodes for supercapacitor due to their high specific surface area and ease of production. The nonwoven mats eliminate the use of binder which not only reduce the surface area but also increase the dead weight.

Different elastoviscous polymers such polyacrylonitrile (PAN), polybenzimidazole (PBI), poly(amic acid) (PAA), cellulose (CA) [103], and polyvinylpyrrolidone (PVP) [104] are used to make CNFs.

The electrospun CNFs still do not have enough specific surface area and thus have low capacitance; however, an activation process can be conducted to increase the surface area. The pristine electrospun CNFs from poly(amide imide) (PAI) have low specific surface area of 240 m^2/g and thus low specific capacitance of 30 F/g and upon activation at 800°C for 1 h in pure carbon dioxide atmosphere the specific surface area increases to 1360 m^2/g resulting in specific capacitance of 196 F/g in KOH electrolyte [45]. Similarly, upon activation of PAN based CNFs using 30 vol% steam in N_2 at 700°C, 1230 m^2/g specific surface area is obtained giving 175 F/g specific capacitance [41]. The PAN based CNFs have specific surface area 850 m^2/g at 800°C which is smaller than the PAI based CNFs made at the same temperature because the micropores in PAN based CNFs turn into mesopores in this atmosphere causing the reduction in surface area.

The surface area can also be increased by using sacrificial polymers which decompose during fabrication process but create pores in the CNFs. The sacrificial polymer is electrospun along with carbon source polymer such as PAN and, upon carbonization, the sacrificial layer will decompose creating pores in the CNFs. The sacrificial layer removes the extra activation step. The weight ratio of these sacrificial polymers also plays an important role and gives maximum surface area at particular weight ratio. Pitch was used as sacrificial polymer and electrospun with PAN (PAN/Pitch 7/3 wt.% (Pitch concentration in THF = 20)) and carbonized at 1000°C. The specific surface area 966.3 m^2/g was obtained which is twice as the area of PAN-CNFs (502 m^2/g). The specific capacitance from PAN/Pitch CNFs was 130 F/g and however the energy and power density were 15 Wh/kg and 100 kW/kg. The maximum capacitance was obtained at Pitch concentration of 20 wt.% in Tetrahydrofuran (THF) which

Table 2: CNTs, open tips, and functionalized CNTs as electrodes for supercapacitors.

Ref	Material type	Growth process	Collector type	Electrolyte	Specific surface area	Specific capacitance	Energy and power density
[24]	MWCNTs,	LPCVD		1 M H_2 SO_4 1 V		79 F/g	1.1 Wh/kg 8.6 MW/kg
[25]	CNTs		Al/Al_2O_3/Fe:Co Al/Al_2O_3/Fe:Mo	$(TEABF_4)$/AN 4 V		25.6 F/g 61.2 F/g	3.56 wh/kg, 2400 kW/kg 8.5 wh/kg, 6580 kW/kg
[26]	Thin Al foil with thin Ni film. MWCNTs growth at 600°C	CVD		1 M H_2SO_4 1 V Organic electrolyte	SSA: 120 m^2/g Pore volume: 0.149 cm^3/g	68 F/g 79 F/g	
[27]	MWCNTs	CVD	Inconel 600	6 M KOH 1.5 V		18 F/g at	7 kW/kg
[28]	AMWCNTS.	CVD	Inconel (600)	$(Et)_4NBF_4$/PC 2.5 V		83 F/g at	0.55 Ω ESR
[29]	SWCNT + PVDF binder.	arc discharge	Raw CNTs Oxidized in air at 300–550°C	6 M KOH 0.8 V	236 m^2/g 644 m^2/g	30 F/g 140 F/g	
[30]	SWCNTs Transferred Cu.	WACVD 750°C	Solid state capacitor	ALD coating of Al_2O_3 and top electrode		23 mF/cm^3 at 20 Hz and 6 mF/cm^3 at 20 kHz.	0.01–0.13 Wh/k
[31]	CNTs on Ni Foam using binder transferred	TCVD 610°C		6 M KOH 0.8 V		25 F/g 9–13 F/g	
[32]	CNTs, No collector or binder.	suspension	On double sided tape	1 M H_2SO_4 1 V		39 F/g	0.02 Wh/kg 5.8 W/kg
[16]	Carbon cloth/CNTs.	MPECVD		neutral PH 0,5 M Na_2SO_4 2 V,	724.8 m^2/g	225 F g^{-1}	28 Wh/kg 87% after 10 k cycles
[33]	MWCNTs transferred on Ni foil	CVD		6 N KOH		21 F g^{-1}	20 kW/kg
[34]	MWCNT. Separated and purified	TCVD At 700°C	Transferred Ni foil.	6 N KOH 1 V		21 F g^{-1}	30 kW/kg

Table 2: Continued.

Ref	Material type	Growth process	Collector type	Electrolyte	Specific surface area	Specific capacitance	Energy and power density
			Open tubes or catalyst removed				
[35]	MWCNTs catalyst removed by HNO_3, functionalized by oxygenation As produced	Arc discharge.		H_2SO_4 1 V	430 m^2/g 250 m^2/g	104 F/g	8 KW/kg. 94 mΩ ESR
[36]	VADWCNTs on CP. Electrochemical oxidation in HNO_3	WACVD		1 M $TEABF_4$/PC. 2.5 V [EMIm][NTf_2] 3 V 1 M $TEABF_4$/PC. 2.5 V [EMIm][NTf_2] 3 V	SSA is 561 m^2/g	66 F/g Organic electrolyte. 75 F/g, 28 F/cm^2 117 F/g 158 F/g, 63 F/cm^2	 27 Wh/kg, 987 kW/kg 52 Wh/kg, 563 kW/kg
[5]	VASWCNTs open tips and side wall windows by heating	WACVD.		Et_4NBF_4/propylene 3.5 V	1300 m^2/g 2240 m^2/g (inner 1180 m^2/g) (outer 1060 m^2/g)	73 F/g, 114 F/g	16 wh/kg 24.7 Wh/g.
[37]	CNTs. Tips opened and N_2- doped	TCVD		1 M KCl 0.7 V		42 F/g. 146 F/g.	
[38]	MWCNT + binder on stainless-steel 500°C in air and microwave treatment Oxygen plasma treated			1 M Na_2SO_4 0.8 V		61.46 F/g, 214.45 F/g 238.23 F/g	
[39]	MWCNTs, Purification and activation + binder CNTs Purification and activation + binder	TCVD	Silica	1 M H_2SO_4 1.4 M $TEABF_4$/AN 2 V 6 M KOH 1 V 1 M H_2SO_4 1.4 M $TEABF_4$/AN (2 V)	1035 m^2/g 885 m^2/g	95 F/g 65 F/g in 90 F/g 85 F/g 65 F/g	
[40]	VAMWCNTs transferred. tip removal O_2 plasma.	TCVD		[EMIM][Tf_2N] IL (4 V).	400 m^2/g.	440 F/g	148 Wh/kg 315 kW/kg

Table 3: Typical properties of carbon nanofibers grown by CVD [20].

Parameter	Typical values
Diameter	1–100 nm
Length	0.1–100 μm
Fill factor when grown as films	5–80%
Density	<2 g/cm^3
Thermal expansion coefficient (CTE)	~10^{-6}/K–10^{-7}/K
Young modulus	80–800 GPa
Electrical resistivity	0.1 $\mu\Omega$·m–2 mΩ·m
Thermal conductivity	20–3000 W/m·K
Temperature tolerance	>1000C without oxygen, >400C with oxygen

is an organic liquid [47]. Similarly, polymethylhydrosiloxane (PMHS) was used as sacrificial polymer with PAN in an organic liquid named Dimethylformamide (DMF). The specific surface area and capacitance were 302 m^2/g and 126 F/g in 6 M KOH electrolyte. The cyclic voltammograms were fairly rectangular showing the complete decomposition of the polymer. High energy density of 10–17 Wh/kg was obtained at high power density of 0.4–20 kW/kg [46]. The pore size can also be controlled by controlling the concentration of sacrificial polymers. Nafion was used as sacrificial polymers for mixtures 60 and 80 wt.% with PAN. The specific surface area of 1614 m^2/g was obtained for 60 wt.% which is four times higher than the SSA of only PAN carbon nanofibers; however, lower surface area of 1499 m^2/g was obtained for 80 wt.%. The mesopore volume (0.810 cm^3/g), cumulative pore volume (1.336 cm^3/g), and pore size (4.69 nm) were higher but the micropores volume was lower than 60 wt.%. Most of the surface area can be accessed due to larger pore diameter. The higher pore volume is due to the higher amount of nafion available for decomposition creating more surface area. The cyclic voltammograms are rectangular even at high scan rate of 2 V/s showing electric double-layer capacitor (EDLC) behavior. The specific capacitances of 210 F/g and 190 F/g were obtained and quite reasonable energy density of 4 Wh/kg is obtained at high power density of 20 kW/kg [50].

Another method to enhance the specific capacitance is the surface modification of the electrode materials which is done by doping with different materials. Nitrogen, oxygen, phosphorous, and boron are used for doping. The doping provides redox reactions, which increase the specific capacitance with some compromise on the power density and lifetime because of slower reaction. Other benefits of doping include the increase in the wettability of electrode material which enhances ion transfer efficiency and the increase in ionic conductivity of materials which decreases IR drop which is the sharp drop in the initial voltage upon discharge due to internal resistance. Yang et al. showed that, with appropriate doping of 3D PAN carbon nanoporous, the resistance can go down from 6.98 Ω to 0.58 Ω [105]. Moreover, CNFs@Ppy were carbonized under nitrogen atmosphere at different temperatures such as 500 to 1100°C which resulted in nitrogen doped CNFs. The maximum SSA 348 m^2/g by carbonization and doping at 900°C was still low but the specific capacitance was 202 F/g which is close to the specific capacitance of activated CNFs with specific surface area of 1500 m^2/g [51]. PAN based CNFs were carbonized in nitrogen atmosphere and doped using oxygen plasma. The contact angle on pristine CNFs about 129° changed to complete wetting. The SSA of pristine and 6-minute plasma treatment was very close to 247 m^2/g and 274 m^2/g; however, the specific capacitance of doped CNFs (377 F/g) was twice as pristine CNFs (167 F/g).

CVD grown CNFs are exclusive in many aspects because they can be grown vertically aligned at different temperatures and controlled location and as an individual fiber or in the form of the film. Their shape, diameter, length, and electrical and mechanical properties can be controlled by the growth conditions and using different metal schemes [106]. The CNFs have the potential to deliver new nanoscale applications and alternate solutions and to cope with future challenges such as NEMs [107], bio sensors [108], interconnects [109], and supercapacitors.

The vertically aligned carbon nanofibers can be grown directly on any kind of substrate by the CVD method. The direct growth on substrate provides metallic contact between substrate and carbon nanofibers which can potentially reduce the equivalent series resistance (ESR) in the supercapacitor. The vertical alignment of CNFs offers the whole surface of CNFs accessible to electrolyte. By this growth technique the CNFs can be grown directly on electrospun CNFs to make composites for further enhancement of the surface area of the electrode along with good electrical contact between both kinds of CNFs as well. These carbon nanofibers can be grown on silicon chips at CMOS compatible temperature (390°C) creating the possibility to fabricate supercapacitor directly on the chip which can be used as decoupling capacitor and ac-bypass capacitor and even to power up of on-chip MEMs devices. Vertically aligned CNFs were grown on silicon chip and the areal specific capacitance of about 5.5 mF/cm^2 was obtained [3, 110]. Nevertheless, the supercapacitors properties based on CNFs electrodes are summarised in Table 4.

5.3. Graphene. Graphene is a two-dimensional material with one atom thick planer sheet of carbon in which atoms are arranged in honeycomb lattice. It is a promising candidate as an electrode for supercapacitor due to high carrier mobility (2×10^5 cm^2 V^{-1} S^{-1}), excellent mechanical properties, and high surface area [111–113]. The theoretical surface area of graphene can be 2630 m^2/g, which can in principle give very high specific capacitance of about 550 F/g [6, 114]. However, postprocessing produces restacking, agglomeration, and damaging of graphene sheets which results in the reduction of surface area and charge mobility of graphene sheet. The measured surface area is lower, ranging from 925 m^2/g to 705 m^2/g and even drops to 46 m^2/g by agglomeration of graphene sheet, which results in low specific capacitance 100 F/g and even lower 6 F/g [54, 55]. Nevertheless, by preventing the agglomeration of graphene sheet, high surface area can be achieved. El-Kady et al. prevented the agglomeration of graphene sheet by reducing the graphene oxide

Table 4: Carbon nanofibers as electrode for supercapacitors.

Ref	Material type	Growth process	Electrolyte	Specific surface area	Specific capacitance	Energy and power density
[41]	CNFs. PAN in DMF Activated in steam	Electrospun	KOH (0.9 V)	1230 m^2/g Micropores 64%	175 F/g	
[42]	ACFF	CVD	1 M H_2SO_4 (0.75 V)	134 m^2/g	146 F/g 10.9 $\mu F/cm^2$	
	CNFs on ACFF		1 M H_2SO_4 0.8 V	784 m^2/g	117 F/g 14.9 $\mu F/cm^2$	
			0.8 M $TEABF_4$ 2 V		34 F/g 4.3 $\mu F/cm^2$	
[43]	CNFs mesoporous and sidewalls openings	Template method	1 M KOH (1.1 V)	1424 m^2/g. Micropore vol. 327 cm^3/g	152 F/	
			1 M $LiClO_4$ in EC/DEC (1 : 1)		70 F/g	
[44]	CNFs on 3D nickel	TCVD	2 M Li_2SO_4 salt.	SSA 500 g/m^2	1.2 F/cm^2. 89.8% after 3000 cycles	2.4 ohm
[45]	CNFs PAI + DMF	Electrospun	1 M H_2SO_4, (1 V)	240 m^2/g	30 F g^{-1}	
	Activated- CNF		6 M KOH	1250 m^2/g Pore size 4–6 nm.	150 F/g 196 F/g	
[46]	CNFs PAN + (PMHS) in DMF	Electrospun	6 M KOH (1 V)	302 m^2/g	127 F/g,	10–17 Wh/kg 0.4–20 kW/kg
[47]	PAN based CNFs	Electrospun.	6 M KOH (1 V).	502 m^2/g, pore vol. 0.1654 cm^3/g, pore size. 17 nm	60 F g^{-1}	6–2 wh/kg 0.1–40 kW/kg.
	PAN/pitch base CNFs			966.3 m^2/g, pore vol.: 0.379 cm^3/g, pore size: 1.573 nm	130.7 F g^{-1}	15.0 Wh/kg 100 kW/kg.
[48]	CNFs On CF/Fe	WA-TCVD	0.5 M Na_2SO_4 (0.7 V)		142 F/g	
[49]	CNFs (PS-b-PEO) + resol opening on walls.	Template		643 m^2/g. Pore vol. 0.157 m^3/g Pore size 2.32 nm	172 F/g	
[50]	PAN based CNFs	Electrospun	0.5 M K_2SO_4 (1 V)	339 m^2/g Mesopores 0.128 cm^3/g	20 F/g,.	
	CNFs PAN + nafion			1499 m^2/g Mesopores 1.336 cm^3/g Pore size. 4.69 nm	210 F/g	4 Wh/kg at 20 kW/kg.
			Doping			
[51]	CNFs@Ppy Annealed at 900°C	Template.		562 m^2/s. Pore volume. 0.51 cm^3/g. Pore size. 3.65 nm	202 F/g.	7.11 Wh/kg 7-8 kW/kg Max. 98 kW/kg 0.14 Ω ESR
[52]	CNFs Bacterial cellulose N, P-codoped		2 M H_2SO_4 (1 V)	289 m^2/g Pore vol.: 0.101 cm^3/g Pore size: 2.21 nm	205 F/g Stable up 4000 cycles.	7.76 Wh/kg. 186 kW/kg. ESR < 1 Ω.
	B, P doped			512 m^2/g Pore vol.: 0.1735 cm^3/g Pore size: 3.64 nm	200 F/g	

Table 4: Continued.

Ref	Material type	Growth process	Electrolyte	Specific surface area	Specific capacitance	Energy and power density
[53]	CNFs PAN + DEF	Electrospun	2 M KOH (1 V).	247 m^2/g Pore volume 0.167 cm^3/g Micropores 0.085 cm^3/g Mesopores 0.082 cm^3/g	167 F/g 129° wetting angle	
	Oxygen plasma treatment			274 m^2/g Pore volume 0.181 cm^3/g Micropore 0.099 cm^3/g Mesopores 0.082 cm^3/g	377 F/g Complete wetting	
[12]	CNFs, PANI on PAN N_2 doped	Electrospun	1 M H_2SO_4	410 m^2/g	335 F/g 86% after 10000 cycles	9.2 Wh/kg 5.8 kW/kg. 4 Ω ESR.
			Gel electrolyte		260 F/g 0.35 F/cm^2 4 F/cm^3	

with laser light by using LightScribe CD/DVD optical drive. High surface area of about 1520 m^2/g was obtained and, however, high specific capacitance of 276 F/g was obtained in EMIMBF4 electrolyte with 4 V scan range. Furthermore, the rate capability of this graphene based capacitor was very high which retained more the 50% area specific capacitance when discharge current density was increased from 1 A/g to 1000 A/g [6]. Graphene based carbon spheres containing both macro- and mesopores were made. The surface area 3290 m^2/g higher than theoretical surface area of the graphene was obtained but the specific capacitance was still low (174 F/g); nevertheless, the energy density (74 Wh/kg) and power density (338 kW/kg) were very high due to presence of mesopores [56]. To further improve the utilization of the surface area of graphene sheets, the spacers were introduced between the graphene layers. The spacer will however increase the volume and the weight of the electrode but it will make the whole surface accessible to the electrolyte and also absence of micropores will result in increase in the power density. The specific capacitance of 273 F/g was obtained with ionic liquid functioning as both electrolyte and spacer. High energy (150 Wh/kg) and power density (776 kW/kg) were obtained [58, 59]. Nevertheless, the supercapacitors' properties based on graphene electrodes are summarised in Table 5.

5.4. Carbon Nanomaterials Composites. The use of carbon nanostructures composites is also investigated as electrode material by increasing the conductivity and accessible surface area. However, the composites of CNTs, CNFs, and graphene are focused here.

The CNTs are the materials with extraordinary electrical properties and can be used to make composite with enhanced electrical conductivity. The high conductivity helped easy charge transfer between pores and surface. The composites of CNTs and PAN nanofibers were made by electrospinning CNTs with PAN followed by carbonization and activation in hydroperoxide at 700°C. The conductivity of the composite (5.32 S cm^{-1}) was higher than only PAN-CNFs (0.86 S cm^{-1}). The specific surface area and specific micropores volume of composite (810 m^2/g) (0.135 cm^3/g) were lower than PAN-CNFs (930 m^2/g) (0.230 cm^3/g) but the mesopores volume of the composite was higher (0.159 cm^3/g) than PAN-CNFs (0.146 cm^3/g). Higher accessible SSA of the composite resulted in higher specific capacitance (310 F/g) than PAN-CNFs (169 F/g). The high mesopores volume also gave high rate capability (90%) when discharge current density was increased from 100 to 1000 mA/g [61]. Similarly, PAN-CNFs and SWCNTs composite was made in similar ways but soaked in HNO_3 to remove metal particles. The SSA obtained from the composite was lower (132 m^2/g) but with higher conductivity (8.82 S cm^{-1}) due to the CNTs. The specific capacitance from the composite was very high (417 F/g) [62]. In addition to embedding by electrospinning, the CNTs are also grown directly on carbon nanofibers by CVD with catalyst particle embedded by electrospinning [22, 63]. Similar to carbon nanotubes, the carbon nanofibers were also used to make composite. The conductivity and SSA of the composite increased when CNFs were used with porous nanosheet from bacterial cellulose. The conductivity of composite increased to 10.1 S m^{-1} compared to nanosheet of 7.6 S m^{-1} [69].

As discussed earlier, graphene is an excellent material as electrode for supercapacitor due to the high electrical conductivity and huge specific surface area, but the agglomeration of graphene sheet causes reduction in surface area; however, their composite with other carbon nanomaterials can enhance both electrical conductivity and specific surface area of overall composite material. The higher conductivity and surface area were observed when graphene

Table 5: Graphene as electrode for supercapacitor.

Ref	Material type	Electrolyte	Specific surface area	Specific capacitance	Energy and power density
[54]	Graphene PTFE binder	KOH (1 V)	705 m^2/g.	135 F/g	
		$TEABF_4$/PC (2.7 V)		94 F/g	
		$TEABF_4$/AN (2.5 V)		99 F/g	
[55]	(EG) exfoliated graphene	1 M H_2SO_4 (1 V)	925 m^2/g	117 F/g 12.4 μF/cm^2	
		PYR_{14}TFSI (3.5 V)		75 F/g	31.9 Wh/kg
	Nanodiamond	1 M H_2SO_4 (1 V)	520 m^2/g	35 F/g 6.7 μF/cm^2	
		PYR_{14}TFSI (3.5 V)		40 F/g	17.0 Wh/kg
	Camphor graphene	1 M H_2SO_4 (1 V)	46 m^2/g	6 F/g	
[6]	Graphene sheet by laser irradiation.	1 M H_3PO_4 (1 V)	1520 m^2/g	3.67 mF/cm^2 96.5% after 10000 cycles.	
		$EMIMBF_4$. (4 V)		276 F/g 5.02 mF/cm^2	
[56]	Graphene Sphere Activated.	[EMIM][TFSI] 3.5 V	3290 m^2/g	174 F/g 100 F/cm^3	74 Wh/kg, 338 kW/kg
		[BMIM][BF_4]/AN		167 F/g 5.6 Ω	
[57]	Pristine graphene	Polymer-gel (PVA-H_3PO_4) electrolyte		80 μF/cm^2	
	Reduced multilayer graphene oxide			247 F/g 394 μF/cm^2	
[58]	Graphene Water as spacer.	H_2SO_4 (1 V)	215 F/g		8 wh/kg 414 KW/kg
		($EMIMBF_4$) (4 V)		273 F/g	150 Wh/kg and 776 kW/kg
[59]	Graphene sheet thermally reduced in water + IL solution which become gel in the end. Gel also works as spacer.	$EMImBF_4$ (3 V)		156 F/g	17.5 Wh/kg
[60]	Exfoliation of graphite in aqueous inorganic salt.				11.3 mF/cm^2

was coated on PAN-nanofibers by spraying graphene oxide. The graphene sheets diffused inside CNFs after carbonization. Little crosslinking of CNFs and graphene resulted in single and few layer graphene sheets with little agglomeration of graphene providing easier access for the electrolyte to the whole surface area. The conductivity of the CNFs/graphene composite (65.9 S m^{-1}) was much higher than CNFs (7.3 S m^{-1}); however, there was a small increase in surface area and pore volume. Similarly, the rate capability of the composite was also very high as compare to CNFs due to high conductivity and easier access of the electrolyte to the surface area. The specific capacitance of the composite dropped only to 155 F/g from 183 F/g when discharging with 10 A/g and 0.1 A/g; however, the drop was huge for CNFs from 114 F/g to 25 F/g [64]. The graphene/CNFs composites were also used to make dense electrode material which can give high volumetric capacitance which is important when the space is limited for the energy source. Phenolic nanofiber/graphene oxide dispersion was ultrasonicated and stirred and finally composite paper was made by vacuum-assisted filtration. The volumetric capacitance higher than commercial capacitor was obtained (112 F cm^{-3}) [65].

The MWCNTs do not disperse in water and aggregate in the bottom; however, the dispersion property of MWCNTs changes to uniform dispersion when mixed with graphene because aromatic regions of graphene oxide sheets interact with the sidewalls of MWCNTs through π-π supramolecular interactions where MWCNTS retain their high conductivity. The MWCNTs were distributed among the graphene layers working as spacers that prevented graphene from agglomeration and also helped the electrolyte to access maximum surface area. Higher surface area from CNTs/graphene

Table 6: One- and two-dimensional carbon nanomaterials composites as electrodes for supercapacitors.

Ref	Material type	Growth process	Electrolyte	Specific surface area	Specific capacitance	Energy and power density
[61]	PAN and MWCNT Carbonization and activation. CNTs exposed	Electrospun	1 M H_2SO_4	810 m^2/g. pore volume 0.294 cm^3/g. micropore, 0.135 cm^3/g. mesopores 0.159 cm^3/g	310 F/g 97% after 1000 cycles.	5.32 S/cm.
[22]	MWCNTs on PAN-CNFs catalyst embedded inside	Electrospun CVD	Gel (0.8 V)		185 F/g at	
[62]	SWCNTs + PAN	Electrospun CVD	6 M KOH (1 V)	132 m^2/g	417 F/g 96% after 2000 cycles	8.82 S/m
[63]	PAN-CNF + CNTS Activation in KOH	CNTs by CVD	1 M NaOH (1 V)	950 m^2/g Pore size 2–40 nm	213 F/g	7.42 Wh/kg 11 Kw/kg
			EMIMBF_4 (4 V)		146 F/g 97% after 20000 cycles	70 wh/kg 8.8 kW/kg,
[17]	Graphene grown on PAN-CNFs carbonization in NH_3N_2 and O_2 doping	Electrospun	1 M Na_2SO_4 (1.8 V)		93% after 5000 cycles	29.1 Wh/kg 7.2 KW/kg.
[64]	GO sprayed on PAN-NFs during electrospinning followed by carbonization	GO diffuse inside CNFs	6 M KOH (0.8 V)	480 m^2/g. Pore volume 0.24 cm^3/g. Pore size 2 nm	183 F/g 38 mF/cm^2 92% after 4500 cycles	65.9 S/cm^1
[65]	Phenolic NF/GO CNFs, carbonization.		6 M KOH (0.9 V)		12 F/cm^3	7.6 S/cm
[66]	Graphene + CNTs on Ti current collector		1 M KCl (1 V)	421 m^2/g Pore size 6.1 nm	72 F/g	
			1 M TEABF_4/PC (3 V)		50 F/g	
			EMI-TFSI IL (4 V)		280 F/g	155 wh/kg 263 kW/kg
[67]	MWCNTs and graphene sheet	CVD	6 M KOH (1 V)		91 F/g	
[68]	MWCNTs + GOs in PAN-CNFs Interlayer distance is 0.8 nm	Electrospun	0.5 M Na_2SO_4 (1 V)	175.1 m^2/g Pore volume 0.156 cm^3/g	120.5 F/g 626 mF/cm^2 109% after 5000 cycles	21.7 S/m
[69]	CNFs-bridged porous carbon by carbonization Activation		6 M KOH	1037 m^2/g pore volume 1.04 cm^3/g	261 F/g 170 F/cm^3 97.6% after 10000 cycles	20.4 Wh/kg at 90 W/kg and 8 Wh/kg at 10 k W/kg 10.1 S/m

($261\,m^2/g$) than only graphene nanosheets ($207\,m^2/g$) is obtained. Similarly, higher specific capacitance of 265 F/g is obtained than graphene nanosheet (200 F/g) [115]. The CNTs/graphene composite was also made using CVD. The specific capacitance of 90 F/g was obtained which was stable up to 5000 cycles [67]. Nevertheless, the supercapacitors properties based on carbon nanomaterials composites electrodes are summarised in Table 6.

6. Conclusion

We have reviewed the use of one- and two-dimensional carbon nanostructures and their composites as electrodes for supercapacitors. Different possibilities to enhance the specific capacitance and of course specific energy and power density are discussed by enhancing surface area, conductivity, hydrophilicity, and doping of carbon nanomaterials. High specific capacitance along with high energy and power density is obtained from CNTs after removing tips and functionalizing with oxygenate. Similarly, results are obtained from graphene by introducing spacer between graphene sheets. The energy density of around 150 Wh/kg and power density of 250–776 kW/kg are obtained.

Competing Interests

The author declares that there is no conflict of interests regarding the publication of this paper.

Acknowledgments

The author would like to acknowledge the financial support of Smoltek AB to carry out this work.

References

[1] V. Desmaris, A. M. Saleem, S. Shafiee, J. Berg, M. S. Kabir, and A. Johansson, "Carbon Nanofibers (CNF) for enhanced solder-based nano-scale integration and on-chip interconnect solutions," in *Proceedings of the 64th Electronic Components and Technology Conference (ECTC '14)*, pp. 1071–1076, Orlando, Fla, USA, May 2014.

[2] V. Desmaris, S. Shafiee, A. M. Saleem, A. Johansson och, and P. Marcoux, "Is it time to reinforce inpackage solder joints using CNFs?" MEPTEC Report, 2014.

[3] A. M. Saleem, G. Göransson, V. Desmaris, and P. Enoksson, "CMOS compatible on-chip decoupling capacitor based on vertically aligned carbon nanofibers," *Solid-State Electronics*, vol. 107, pp. 15–19, 2015.

[4] V. Desmaris, A. M. Saleem, J. Berg et al., "A test vehicle for RF/DC evaluation and destructive testing of vertically grown nanostructures (VGCNS)," in *Proceedings of the International Conference on the Science and Application of Nanotubes (NT '11)*, Cambridge, UK, July 2011.

[5] T. Hiraoka, A. Izadi-Najafabadi, T. Yamada et al., "Compact and light supercapacitor electrodes from a surface-only solid by opened carbon nanotubes with 2 200 $m_2\ g^{-1}$ surface area," *Advanced Functional Materials*, vol. 20, no. 3, pp. 422–428, 2010.

[6] M. F. El-Kady, V. Strong, S. Dubin, and R. B. Kaner, "Laser scribing of high-performance and flexible graphene-based electrochemical capacitors," *Science*, vol. 335, no. 6074, pp. 1326–1330, 2012.

[7] M. S. Halper och and J. C. Ellenbogen, *Supercapacitors: A Brief Overview*, MITRE Nanosystems Group, McLean, Va, USA, 2006.

[8] T. A. Smith, J. P. Mars, and G. A. Turner, "Using supercapacitors to improve battery performance," in *Proceedings of the IEEE 33rd Annual Power Electronics Specialists Conference (PESC '02)*, vol. 1, pp. 124–128, Cairns, Australia, June 2002.

[9] H. Hõimoja, D. Vinnikov, and T. Jalakas, "Analysis and design of ultracapacitor-boosted back-up power supply for tramcars," in *Proceedings of IEEE EUROCON*, pp. 583–589, Saint Petersburg, Russia, May 2009.

[10] T. Olivo, "Analysis of ultra capacitors as UPS energy storage devices," in *Proceedings of the IEEE Southeast Conference*, pp. 398–401, Concord, NC, USA, March 2010.

[11] J. R. Miller and P. Simon, "Electrochemical capacitors for energy management," *Science*, vol. 321, no. 5889, pp. 651–652, 2008.

[12] F. Miao, C. Shao, X. Li, K. Wang, and Y. Liu, "Flexible solid-state supercapacitors based on freestanding nitrogen-doped porous carbon nanofibers derived from electrospun polyacrylonitrile@polyaniline nanofibers," *Journal of Materials Chemistry A*, vol. 4, no. 11, pp. 4180–4187, 2016.

[13] G. Wang, L. Zhang, and J. Zhang, "A review of electrode materials for electrochemical supercapacitors," *Chemical Society Reviews*, vol. 41, no. 2, pp. 797–828, 2012.

[14] M. P. Bichat, E. Raymundo-Piñero, and F. Béguin, "High voltage supercapacitor built with seaweed carbons in neutral aqueous electrolyte," *Carbon*, vol. 48, no. 15, pp. 4351–4361, 2010.

[15] C. Vix-Guterl, E. Frackowiak, K. Jurewicz, M. Friebe, J. Parmentier, and F. Béguin, "Electrochemical energy storage in ordered porous carbon materials," *Carbon*, vol. 43, no. 6, pp. 1293–1302, 2005.

[16] Y.-K. Hsu, Y.-C. Chen, Y.-G. Lin, L.-C. Chen, and K.-H. Chen, "High-cell-voltage supercapacitor of carbon nanotube/carbon cloth operating in neutral aqueous solution," *Journal of Materials Chemistry*, vol. 22, no. 8, pp. 3383–3387, 2012.

[17] L. Zhao, Y. Qiu, J. Yu, X. Deng, C. Dai, and X. Bai, "Carbon nanofibers with radially grown graphene sheets derived from electrospinning for aqueous supercapacitors with high working voltage and energy density," *Nanoscale*, vol. 5, no. 11, pp. 4902–4909, 2013.

[18] P. Huang, D. Pech, R. Lin et al., "On-chip micro-supercapacitors for operation in a wide temperature range," *Electrochemistry Communications*, vol. 36, pp. 53–56, 2013.

[19] B.-H. Kim, K. S. Yang, and J. P. Ferraris, "Highly conductive, mesoporous carbon nanofiber web as electrode material for high-performance supercapacitors," *Electrochimica Acta*, vol. 75, pp. 325–331, 2012.

[20] V. Desmaris, M. A. Saleem, and S. Shafiee, "Examining carbon nanofibers: properties, growth, and applications," *IEEE Nanotechnology Magazine*, vol. 9, no. 2, pp. 33–38, 2015.

[21] A. Luzio, E. V. Canesi, C. Bertarelli, and M. Caironi, "Electrospun polymer fibers for electronic applications," *Materials*, vol. 7, no. 2, pp. 906–947, 2014.

[22] Z. Zhou, X.-F. Wu, and H. Fong, "Electrospun carbon nanofibers surface-grafted with vapor-grown carbon nanotubes as hierarchical electrodes for supercapacitors," *Applied Physics Letters*, vol. 100, no. 2, Article ID 023115, 2012.

[23] F. Béguin och and E. Frąckowiak, *I Supercapacitor Materials, System, and Applications*, WILEY-VCH Verlag GmbH & Co. KGaA, 2013.

[24] R. Reit, J. Nguyen, and W. J. Ready, "Growth time performance dependence of vertically aligned carbon nanotube supercapacitors grown on aluminum substrates," *Electrochimica Acta*, vol. 91, pp. 96–100, 2013.

[25] S. Dörfler, I. Felhösi, T. Marek et al., "High power supercap electrodes based on vertical aligned carbon nanotubes on aluminum," *Journal of Power Sources*, vol. 227, pp. 218–228, 2013.

[26] R. Kavian, A. Vicenzo, and M. Bestetti, "Growth of carbon nanotubes on aluminium foil for supercapacitors electrodes," *Journal of Materials Science*, vol. 46, no. 5, pp. 1487–1493, 2011.

[27] S. Talapatra, S. Kar, S. K. Pal et al., "Direct growth of aligned carbon nanotubes on bulk metals," *Nature Nanotechnology*, vol. 1, no. 2, pp. 112–116, 2006.

[28] L. Gao, A. Peng, Z. Y. Wang et al., "Growth of aligned carbon nanotube arrays on metallic substrate and its application to supercapacitors," *Solid State Communications*, vol. 146, no. 9-10, pp. 380–383, 2008.

[29] F. Picó, J. M. Rojo, M. L. Sanjuán et al., "Single-walled carbon nanotubes as electrodes in supercapacitors," *Journal of the Electrochemical Society*, vol. 151, no. 6, pp. A831–A837, 2004.

[30] C. L. Pint, N. W. Nicholas, S. Xu et al., "Three dimensional solid-state supercapacitors from aligned single-walled carbon nanotube array templates," *Carbon*, vol. 49, no. 14, pp. 4890–4897, 2011.

[31] R. Shi, L. Jiang, and C. Pan, "A single-step process for preparing supercapacitor electrodes from carbon nanotubes," *Soft Nanoscience Letters*, vol. 1, no. 1, pp. 11–15, 2011.

[32] M. Kaempgen, J. Ma, G. Gruner, G. Wee, and S. G. Mhaisalkar, "Bifunctional carbon nanotube networks for supercapacitors," *Applied Physics Letters*, vol. 90, no. 26, Article ID 264104, 2007.

[33] C. Du and N. Pan, "High power density supercapacitor electrodes of carbon nanotube films by electrophoretic deposition," *Nanotechnology*, vol. 17, no. 21, pp. 5314–5318, 2006.

[34] C. Du, J. Yeh, and N. Pan, "High power density supercapacitors using locally aligned carbon nanotube electrodes," *Nanotechnology*, vol. 16, no. 4, pp. 350–353, 2005.

[35] C. Niu, E. K. Sichel, R. Hoch, D. Moy, and H. Tennent, "High power electrochemical capacitors based on carbon nanotube electrodes," *Applied Physics Letters*, vol. 70, no. 11, pp. 1480–1482, 1997.

[36] B. Kim, H. Chung, and W. Kim, "High-performance supercapacitors based on vertically aligned carbon nanotubes and nonaqueous electrolytes," *Nanotechnology*, vol. 23, no. 15, Article ID 155401, 2012.

[37] A. R. John and P. Arumugam, "Open ended nitrogen-doped carbon nanotubes for the electrochemical storage of energy in a supercapacitor electrode," *Journal of Power Sources*, vol. 277, pp. 387–392, 2015.

[38] P. Dulyaseree, V. Yordsri, and W. Wongwiriyapan, "Effects of microwave and oxygen plasma treatments on capacitive characteristics of supercapacitor based on multiwalled carbon nanotubes," *Japanese Journal of Applied Physics*, vol. 55, no. 2, Article ID 02BD05, 2016.

[39] E. Frackowiak, S. Delpeux, K. Jurewicz, K. Szostak, D. Cazorla-Amoros, and F. Béguin, "Enhanced capacitance of carbon nanotubes through chemical activation," *Chemical Physics Letters*, vol. 361, no. 1-2, pp. 35–41, 2002.

[40] W. Lu, L. Qu, K. Henry, and L. Dai, "High performance electrochemical capacitors from aligned carbon nanotube electrodes and ionic liquid electrolytes," *Journal of Power Sources*, vol. 189, no. 2, pp. 1270–1277, 2009.

[41] C. Kim and K. S. Yang, "Electrochemical properties of carbon nanofiber web as an electrode for supercapacitor prepared by electrospinning," *Applied Physics Letters*, vol. 83, no. 6, pp. 1216–1218, 2003.

[42] T.-H. Ko, K.-H. Hung, S.-S. Tzeng, J.-W. Shen Och, and C.-H. Hung, "Carbon nanofibers grown on activated carbon fiber fabrics as electrode of supercapacitors," *Physica Scripta*, vol. 129, pp. 80–84, 2007.

[43] K. Wang, Y. Wang, Y. Wang, E. Hosono, and H. Zhou, "Mesoporous carbon nanofibers for supercapacitor application," *Journal of Physical Chemistry C*, vol. 113, no. 3, pp. 1093–1097, 2009.

[44] J. R. McDonough, J. W. Choi, Y. Yang, F. La Mantia, Y. Zhang, and Y. Cui, "Carbon nanofiber supercapacitors with large areal capacitances," *Applied Physics Letters*, vol. 95, no. 24, Article ID 243109, 2009.

[45] M.-K. Seo and S.-J. Park, "Electrochemical characteristics of activated carbon nanofiber electrodes for supercapacitors," *Materials Science and Engineering: B*, vol. 164, no. 2, pp. 106–111, 2009.

[46] B.-H. Kim, K. S. Yang, H.-G. Woo, and K. Oshida, "Supercapacitor performance of porous carbon nanofiber composites prepared by electrospinning polymethylhydrosiloxane (PMHS)/polyacrylonitrile (PAN) blend solutions," *Synthetic Metals*, vol. 161, no. 13-14, pp. 1211–1216, 2011.

[47] B.-H. Kim, K. S. Yang, Y. A. Kim, Y. J. Kim, B. An, and K. Oshida, "Solvent-induced porosity control of carbon nanofiber webs for supercapacitor," *Journal of Power Sources*, vol. 196, no. 23, pp. 10496–10501, 2011.

[48] Y. Gao, G. P. Pandey, J. Turner, C. R. Westgate, and B. Sammakia, "Chemical vapor-deposited carbon nanofibers on carbon fabric for supercapacitor electrode applications," *Nanoscale Research Letters*, vol. 7, article 651, 2012.

[49] E. Kang, G. Jeon, and J. K. Kim, "Free-standing, well-aligned ordered mesoporous carbon nanofibers on current collectors for high-power micro-supercapacitors," *Chemical Communications*, vol. 49, no. 57, pp. 6406–6408, 2013.

[50] C. Tran and V. Kalra, "Fabrication of porous carbon nanofibers with adjustable pore sizes as electrodes for supercapacitors," *Journal of Power Sources*, vol. 235, pp. 289–296, 2013.

[51] L.-F. Chen, X.-D. Zhang, H.-W. Liang et al., "Synthesis of nitrogen-doped porous carbon nanofibers as an efficient electrode material for supercapacitors," *ACS Nano*, vol. 6, no. 8, pp. 7092–7102, 2012.

[52] L.-F. Chen, Z.-H. Huang, H.-W. Liang, H.-L. Gao, and S.-H. Yu, "Three-dimensional heteroatom-doped carbon nanofiber networks derived from bacterial cellulose for supercapacitors," *Advanced Functional Materials*, vol. 24, no. 32, pp. 5104–5111, 2014.

[53] C.-C. Lai and C.-T. Lo, "Plasma oxidation of electrospun carbon nanofibers as supercapacitor electrodes," *RSC Advances*, vol. 5, no. 49, pp. 38868–38872, 2015.

[54] M. D. Stoller, S. Park, Z. Yanwu, J. An, and R. S. Ruoff, "Graphene-based ultracapacitors," *Nano Letters*, vol. 8, no. 10, pp. 3498–3502, 2008.

[55] S. R. C. Vivekchand, C. S. Rout, K. S. Subrahmanyam, A. Govindaraj, and C. N. R. Rao, "Graphene-based electrochemical supercapacitors," *Journal of Chemical Sciences*, vol. 120, no. 1, pp. 9–13, 2008.

[56] T. Kim, G. Jung, S. Yoo, K. S. Suh, and R. S. Ruoff, "Activated graphene-based carbons as supercapacitor electrodes with macro- and mesopores," *ACS Nano*, vol. 7, no. 8, pp. 6899–6905, 2013.

[57] J. J. Yoo, K. Balakrishnan, J. Huang et al., "Ultrathin planar graphene supercapacitors," *Nano Letters*, vol. 11, no. 4, pp. 1423–1427, 2011.

[58] X. Yang, J. Zhu, L. Qiu, and D. Li, "Bioinspired effective prevention of restacking in multilayered graphene films: towards the next generation of high-performance supercapacitors," *Advanced Materials*, vol. 23, no. 25, pp. 2833–2838, 2011.

[59] M. A. Pope, S. Korkut, C. Punckt, and I. A. Aksay, "Supercapacitor electrodes produced through evaporative consolidation of graphene oxide-water-ionic liquid gels," *Journal of the Electrochemical Society*, vol. 160, no. 10, pp. A1653–A1660, 2013.

[60] K. Parvez, Z.-S. Wu, R. Li et al., "Exfoliation of graphite into graphene in aqueous solutions of inorganic salts," *Journal of the American Chemical Society*, vol. 136, no. 16, pp. 6083–6091, 2014.

[61] Q. Guo, X. Zhou, X. Li et al., "Supercapacitors based on hybrid carbon nanofibers containing multiwalled carbon nanotubes," *Journal of Materials Chemistry*, vol. 19, no. 18, pp. 2810–2816, 2009.

[62] L. Cheng, J. He, Y. Jin, H. Chen, and M. Chen, "Single-walled carbon nanotube embedded porous carbon nanofiber with enhanced electrochemical capacitive performance," *Materials Letters*, vol. 144, pp. 123–126, 2015.

[63] Y. Qiu, G. Li, Y. Hou et al., "Vertically aligned carbon nanotubes on carbon nanofibers: a hierarchical three-dimensional carbon nanostructure for high-energy flexible supercapacitors," *Chemistry of Materials*, vol. 27, no. 4, pp. 1194–1200, 2015.

[64] Q. Dong, G. Wang, H. Hu et al., "Ultrasound-assisted preparation of electrospun carbon nanofiber/graphene composite electrode for supercapacitors," *Journal of Power Sources*, vol. 243, pp. 350–353, 2013.

[65] C. Ma, X. Wang, Y. Ma et al., "Carbon nanofiber/graphene composite paper for flexible supercapacitors with high volumetric capacitance," *Materials Letters*, vol. 145, pp. 197–200, 2015.

[66] Q. Cheng, J. Tang, J. Ma, H. Zhang, N. Shinya, and L.-C. Qin, "Graphene and carbon nanotube composite electrodes for supercapacitors with ultra-high energy density," *Physical Chemistry Chemical Physics*, vol. 13, no. 39, pp. 17615–17624, 2011.

[67] C.-C. Lin and Y.-W. Lin, "Synthesis of carbon nanotube/graphene composites by one-step chemical vapor deposition for electrodes of electrochemical capacitors," *Journal of Nanomaterials*, vol. 2015, Article ID 741928, 8 pages, 2015.

[68] H.-C. Hsu, C.-H. Wang, Y.-C. Chang, J.-H. Hu, B.-Y. Yao, and C.-Y. Lin, "Graphene oxides and carbon nanotubes embedded in polyacrylonitrile-based carbon nanofibers used as electrodes for supercapacitor," *Journal of Physics and Chemistry of Solids*, vol. 85, pp. 62–68, 2015.

[69] Y. Jiang, J. Yan, X. Wu et al., "Facile synthesis of carbon nanofibers-bridged porous carbon nanosheets for high-performance supercapacitors," *Journal of Power Sources*, vol. 307, pp. 190–198, 2016.

[70] E. Pop, D. Mann, Q. Wang, K. Goodson, and H. Dai, "Thermal conductance of an individual single-wall carbon nanotube above room temperature," *Nano Letters*, vol. 6, no. 1, pp. 96–100, 2006.

[71] S. Hong and S. Myung, "Nanotube electronics: a flexible approach to mobility," *Nature Nanotechnology*, vol. 2, no. 4, pp. 207–208, 2007.

[72] M.-F. Yu, B. S. Files, S. Arepalli, and R. S. Ruoff, "Tensile loading of ropes of single wall carbon nanotubes and their mechanical properties," *Physical Review Letters*, vol. 84, no. 24, pp. 5552–5555, 2000.

[73] D. S. Lee, J. Svensson, S. W. Lee, Y. W. Park, and E. E. B. Campbell, "Fabrication of crossed junctions of semiconducting and metallic carbon nanotubes: a CNT-gated CNT-FET," *Journal of Nanoscience and Nanotechnology*, vol. 6, no. 5, pp. 1325–1330, 2006.

[74] X. Liu, S. Han, and C. Zhou, "Novel Nanotube-on-Insulator (NOI) approach toward single-walled carbon nanotube devices," *Nano Letters*, vol. 6, no. 1, pp. 34–39, 2006.

[75] D. Shahrjerdi, A. D. Franklin, S. Oida, J. A. Ott, G. S. Tulevski, and W. Haensch, "High-performance air-stable n-type carbon nanotube transistors with erbium contacts," *ACS Nano*, vol. 7, no. 9, pp. 8303–8308, 2013.

[76] A. Javey, J. Guo, Q. Wang, M. Lundstrom, and H. Dai, "Ballistic carbon nanotube field-effect transistors," *Nature*, vol. 424, no. 6949, pp. 654–657, 2003.

[77] F. Kreupl, A. P. Graham, G. S. Duesberg et al., "Carbon nanotubes in interconnect applications," *Microelectronic Engineering*, vol. 64, no. 1–4, pp. 399–408, 2002.

[78] B. Q. Wei, R. Vajtai, and P. M. Ajayan, "Reliability and current carrying capacity of carbon nanotubes," *Applied Physics Letters*, vol. 79, no. 8, pp. 1172–1174, 2001.

[79] J. Kong, N. R. Franklin, C. Zhou et al., "Nanotube molecular wires as chemical sensors," *Science*, vol. 287, no. 5453, pp. 622–625, 2000.

[80] J. T. W. Yeow and Y. Wang, "A review of carbon nanotubes-based gas sensors," *Journal of Sensors*, vol. 2009, Article ID 493904, 24 pages, 2009.

[81] Y. Fu, N. Nabiollahi, T. Wang et al., "A complete carbon-nanotube-based on-chip cooling solution with very high heat dissipation capacity," *Nanotechnology*, vol. 23, no. 4, Article ID 045304, 2012.

[82] X. Wang, Q. Li, J. Xie et al., "Fabrication of ultralong and electrically uniform single-walled carbon nanotubes on clean substrates," *Nano Letters*, vol. 9, no. 9, pp. 3137–3141, 2009.

[83] L. Schlapbach and A. Züttel, "Hydrogen-storage materials for mobile applications," *Nature*, vol. 414, no. 6861, pp. 353–358, 2001.

[84] Z. Shi, Y. Lian, X. Zhou et al., "Mass-production of single-wall carbon nanotubes by arc discharge method," *Carbon*, vol. 37, no. 9, pp. 1449–1453, 1999.

[85] M. Jinno, S. Bandow, and Y. Ando, "Multiwalled carbon nanotubes produced by direct current arc discharge in hydrogen gas," *Chemical Physics Letters*, vol. 398, no. 1–3, pp. 256–259, 2004.

[86] A. Thess, R. Lee, P. Nikolaev et al., "Crystalline ropes of metallic carbon nanotubes," *Science*, vol. 273, no. 5274, pp. 483–487, 1996.

[87] X. Zhao, M. Ohkohchi, M. Wang, S. Iijima, T. Ichihashi, and Y. Ando, "Preparation of high-grade carbon nanotubes by hydrogen arc discharge," *Carbon*, vol. 35, no. 6, pp. 775–781, 1997.

[88] A. M. Saleem, S. Rahiminejad, V. Desmaris, and P. Enoksson, "Carbon nanotubes as base material for fabrication of gap waveguide components," *Sensors and Actuators A: Physical*, vol. 224, pp. 163–168, 2015.

[89] L. Samandari-Masouleh, N. Mostoufi, A. Khodadadi, Y. Mortazavi, and M. Maghrebi, "Modeling the growth of carbon nanotubes in a floating catalyst reactor," *Industrial and Engineering Chemistry Research*, vol. 51, no. 3, pp. 1143–1149, 2012.

[90] K. Dasgupta, S. Kar, R. Venugopalan et al., "Self-standing geometry of aligned carbon nanotubes with high surface area," *Materials Letters*, vol. 62, no. 12-13, pp. 1989–1992, 2008.

[91] R. Bhowmick, B. M. Clemens, and B. A. Cruden, "Parametric analysis of chirality families and diameter distributions in single-wall carbon nanotube production by the floating catalyst method," *Carbon*, vol. 46, no. 6, pp. 907–922, 2008.

[92] K. Hata, D. N. Futaba, K. Mizuno, T. Namai, M. Yumura, and S. Iijima, "Water-assisted highly efficient synthesis of impurity-free single-walled carbon nanotubes," *Science*, vol. 306, no. 5700, pp. 1362–1364, 2004.

[93] Q. Li, X. Zhang, R. F. DePaula et al., "Sustained growth of ultralong carbon nanotube arrays for fiber spinning," *Advanced Materials*, vol. 18, no. 23, pp. 3160–3163, 2006.

[94] S. Chakrabarti, T. Nagasaka, Y. Yoshikawa, L. Pan, and Y. Nakayama, "Growth of super long aligned brush-like carbon nanotubes," *Japanese Journal of Applied Physics*, vol. 45, no. 24–28, pp. L720–L722, 2006.

[95] M. S. A. Bistamam, M. A. Azam, N. S. A. Manaf, P. S. Goh, M. W. A. Rashid, and A. F. Ismail, "An overview of selected catalytic chemical vapor deposition parameter for aligned carbon nanotube growth," *Nanoscience and Nanotechnology Asia*, vol. 4, no. 1, pp. 2–30, 2014.

[96] J. Y. Lee, K. H. An, J. K. Heo, and Y. H. Lee, "Fabrication of supercapacitor electrodes using fluorinated single-walled carbon nanotubes," *The Journal of Physical Chemistry B*, vol. 107, no. 34, pp. 8812–8815, 2003.

[97] B. Zhang, J. Liang, C. L. Xu, B. Q. Wei, D. B. Ruan, and D. H. Wu, "Electric double-layer capacitors using carbon nanotube electrodes and organic electrolyte," *Materials Letters*, vol. 51, no. 6, pp. 539–542, 2001.

[98] L. Staaf, A. M. Saleem, G. Göransson, M. Haque, P. Lundgren Och, and P. Enoksson, "Carbon nanotubes as electrode for supercapacitors," in *Proceedings of the 2nd International Conference on Materials for Energy—EnMat II*, Karlsruhe, Germany, 2013.

[99] E. Kao, C. Yang, R. Warren, A. Kozinda, and L. Lin, "ALD titanium nitride coated carbon nanotube electrodes for electrochemical supercapacitors," in *Proceedings of the 18th International Conference on Solid-State Sensors, Actuators and Microsystems (TRANSDUCERS '15)*, pp. 498–501, Anchorage, Alaska, USA, June 2015.

[100] Y. Rangom, X. Tang, and L. F. Nazar, "Carbon nanotube-based supercapacitors with excellent ac line filtering and rate capability via improved interfacial impedance," *ACS Nano*, vol. 9, no. 7, pp. 7248–7255, 2015.

[101] Y. Yoo, S. Kim, B. Kim, and W. Kim, "2.5 V compact supercapacitors based on ultrathin carbon nanotube films for AC line filtering," *Journal of Materials Chemistry A*, vol. 3, no. 22, pp. 11801–11806, 2015.

[102] G. Fiorentino, S. Vollebregt, F. D. Tichelaar, R. Ishihara, and P. M. Sarro, "Impact of the atomic layer deposition precursors diffusion on solid-state carbon nanotube based supercapacitors performances," *Nanotechnology*, vol. 26, no. 6, Article ID 064002, 2015.

[103] V. Kuzmenko, A. M. Saleem, O. Naboka et al., "Carbon nanotubes/nanofibers composites from cellulose for supercapacitors," in *Proceedings of the 16th European Conference on Composite Materials (ECCM '14)*, Seville, Spain, June 2014.

[104] P. Wang, D. Zhang, F. Ma et al., "Mesoporous carbon nanofibers with a high surface area electrospun from thermoplastic polyvinylpyrrolidone," *Nanoscale*, vol. 4, no. 22, pp. 7199–7204, 2012.

[105] X. Yang, D. Wu, X. Chen, and R. Fu, "Nitrogen-enriched nanocarbons with a 3-D continuous mesopore structure from polyacrylonitrile for supercapacitor application," *The Journal of Physical Chemistry C*, vol. 114, no. 18, pp. 8581–8586, 2010.

[106] J. Yun, R. Wang, W. K. Choi et al., "Field emission from a large area of vertically-aligned carbon nanofibers with nanoscale tips and controlled spatial geometry," *Carbon*, vol. 48, no. 5, pp. 1362–1368, 2010.

[107] B. A. Cruden and A. M. Cassell, "Vertically oriented carbon nanofiber based nanoelectromechanical switch," *IEEE Transactions on Nanotechnology*, vol. 5, no. 4, pp. 350–355, 2006.

[108] K. A. Al Mamun, F. S. Tulip, K. MacArthur, N. McFarlane, S. K. Islam, and D. Hensley, "Vertically aligned carbon nanofiber based biosensor platform for glucose sensor," *International Journal of High Speed Electronics and Systems*, vol. 23, no. 1-2, Article ID 1450006, 2014.

[109] Q. Ngo, T. Yamada, M. Suzuki et al., "Structural and electrical characterization of carbon nanofibers for interconnect via applications," *IEEE Transactions on Nanotechnology*, vol. 6, no. 6, pp. 688–695, 2007.

[110] A. M. Saleem, S. Shafiee, T. Krasia-Christoforou et al., "Low temperature and cost-effective growth of vertically aligned carbon nanofibers using spin-coated polymer-stabilized palladium nanocatalysts," *Science and Technology of Advanced Materials*, vol. 16, no. 1, Article ID 015007, 2015.

[111] K. I. Bolotin, K. J. Sikes, Z. Jiang et al., "Ultrahigh electron mobility in suspended graphene," *Solid State Communications*, vol. 146, no. 9-10, pp. 351–355, 2008.

[112] Y. Gao, Y. S. Zhou, W. Xiong et al., "Transparent, flexible, and solid-state supercapacitors based on graphene electrodes," *APL Materials*, vol. 1, no. 1, Article ID 012101, 2013.

[113] C. Xu, B. Xu, Y. Gu, Z. Xiong, J. Sun, and X. S. Zhao, "Graphene-based electrodes for electrochemical energy storage," *Energy & Environmental Science*, vol. 6, no. 6, pp. 1388–1414, 2013.

[114] Y. Zhu, S. Murali, W. Cai et al., "Graphene and graphene oxide: synthesis, properties, and applications," *Advanced Materials*, vol. 22, no. 35, pp. 3906–3924, 2010.

[115] X. Lu, H. Dou, B. Gao et al., "A flexible graphene/multiwalled carbon nanotube film as a high performance electrode material for supercapacitors," *Electrochimica Acta*, vol. 56, no. 14, pp. 5115–5121, 2011.